Spatiotemporal Structure of Pulsating Solitons in the Cubic–Quintic Ginzburg–Landau Equation: A Novel Variational Formulation

Stefan C. Mancas and S. Roy Choudhury
Department of Mathematics
University of Central Florida
Orlando, FL 32816–1364
mancass@erau.edu
choudhur@longwood.cs.ucf.edu

Abstract

Comprehensive numerical simulations (reviewed in Dissipative Solitons, Akhmediev and Ankiewicz (Eds.), Springer, Berlin, 2005) of pulse solutions of the cubic–quintic Ginzburg–Landau Equation (CGLE), a canonical equation governing the weakly nonlinear behavior of dissipative systems in a wide variety of disciplines, reveal various intriguing and entirely novel classes of solutions. In particular, there are five new classes of pulse or solitary waves solutions, viz. pulsating, creeping, snake, erupting, and chaotic solitons. In contrast to the regular solitary waves investigated in numerous integrable and non–integrable systems over the last three decades, these dissipative solitons are not stationary in time. Rather, they are spatially confined pulse–type structures whose envelopes exhibit complicated temporal dynamics. The numerical simulations also reveal very interesting bifurcations sequences of these pulses as the parameters of the CGLE are varied.

In this paper, we address the issues of central interest in the area, i.e., the conditions for the occurrence of the five categories of dissipative solitons, as well the dependence of both their shape and their stability on the various parameters of the CGLE, viz. the nonlinearity, dispersion, linear and nonlinear gain, loss and spectral filtering parameters. Our predictions on the variation of the soliton amplitudes, widths and periods with the CGLE parameters agree with simulation results.

First, we elucidate the Hopf bifurcation mechanism responsible for the various pulsating solitary waves, as well as its absence in Hamiltonian and integrable systems where such structures are absent. Next, we develop and discuss a variational formalism within which to explore the various classes of dissipative solitons. Given the complex dynamics of the various dissipative solutions, this formulation is, of necessity, significantly generalized over all earlier approaches in several crucial ways. Firstly, the starting formulation for the Lagrangian is recent and not well explored. Also, the trial functions have been generalized considerably over conventional ones to keep the shape relatively simple (and the trial function integrable!) while allowing arbitrary temporal variation of the amplitude, width, position, speed and phase of the pulses.

In addition, the resulting Euler–Lagrange equations are treated in a completely novel way. Rather than consider the stable fixed points which correspond to the well–known stationary solitons or plain pulses, we use dynamical systems theory to focus on more complex attractors viz. periodic, quasiperiodic, and chaotic ones. Periodic evolution of the trial function parameters on stable periodic attractors yield solitons whose amplitudes and widths are non–stationary or time dependent. In particular, pulsating and snake dissipative solitons may be treated in this manner. Detailed results are presented here for the pulsating solitary waves — their regimes of occurrence, bifurcations, and the parameter dependences of the amplitudes, widths, and periods agree with simulation results. Snakes and chaotic solitons will be addressed in subsequent papers. This overall approach fails only to address the fifth class of dissipative solitons, viz. the exploding or erupting solitons.

1 Introduction

The cubic–quintic complex Ginzburg–Landau equation (CGLE) is the canonical equation governing the weakly nonlinear behavior of dissipative systems in a wide variety of disciplines [1]. In fluid mechanics, it is also often referred to as the Newell–Whitehead equation after the authors who derived it in the context of Bénard convection [1, 2].

As such, it is also one of the most widely studied nonlinear equations. Many basic properties of the equation and its solutions are reviewed in [3, 4], together with applications to a vast variety of phenomena including nonlinear waves, second–order phase transitions, superconductivity, superfluidity, Bose–Einstein condensation, liquid crystals and string theory. The numerical studies by Brusch et al [5, 6] which primarily consider periodic traveling wave solutions of the cubic CGLE, together with secondary pitchfork bifurcations and period doubling cascades into disordered turbulent regimes, also give comprehensive summaries of other work on this system. Early numerical studies [7, 8] and theoretical investigations [9, 10] of periodic solutions and secondary bifurcations are also of general interest for our work here.

Certain situations or phenomena, such as where the cubic nonlinear term is close to zero, may require the inclusion of higher–order nonlinearities leading to the so–called cubic–quintic CGLE [11]. This has proved to be a rich system with very diverse solution behaviors. In particular, a relatively early and influential review by van Saarloos and Hohenberg, also recently extended to two coupled cubic CGL equations [12, 13], considered phase–plane counting arguments for traveling wave coherent structures, some analytic and perturbative solutions, limited comparisons to numerics, and so–called "linear marginal stability analysis" to select the phase speed of the traveling waves.

Among the multitude of other papers, we shall only refer to two sets of studies which will directly pertain to the work in this article. The first class of papers [14–18] used dynamical systems techniques to prove that the cubic–quintic CGLE admits periodic and quasi–periodic traveling wave solutions.

The second class of papers [19, 20], primarily involving numerical simulations of the full cubic–quintic CGL PDE in the context of Nonlinear Optics, revealed various branches of plane wave solutions which are referred to as continuous wave (CW) solutions in the Optics literature. More importantly, these latter studies also found various spatially confined coherent structures of the PDE, with envelopes which exhibit complicated temporal dynamics. In [20], these various structures are categorized as plain pulses (or regular stationary

solutions), pulsating solitary waves, creeping solitons, slugs or snakes, erupting solitons, and chaotic solitons depending on the temporal behavior of the envelopes. In addition, note that the speed of the new classes of solutions may be zero, constant, or periodic (since it is determined by boundary conditions, the speed is an eigenvalue, and it may be in principle also quasiperiodic or chaotic, although no such cases appear to have been reported). All indications are that these classes of solutions, all of which have amplitudes which vary in time, do not exist as stable structures in Hamiltonian systems. Even if excited initially, amplitude modulated solitary waves restructure into regular stationary solutions [21]. Exceptions to this rule are the integrable models where the pulsating structures are nonlinear superpositions or fundamental solutions [22]. Hence, these classes of solutions are novel and they exist only in the presence of dissipation in the simulations of [20]. Also, secondary complete period doubling cascades of the pulsating solitons leading as usual to regimes of chaos are also found. This last feature for numerical solutions of the full cubic–quintic PDE is strongly reminiscent of the period doubling cascades found in [5, 6] for period solutions of the traveling wave reduced ODEs of the cubic CGLE.

In this context, we note that numerous attempts have been made to extend the well–developed concept of soliton interactions in integrable, conservative systems [23] to more realistic active or dissipative media which are governed by non–integrable model equations. The reason is that the complicated spatio–temporal dynamics of such coherent structure solutions are governed by simple systems of ordinary differential equations, or low–dimensional dynamical systems, rather by the original complex nonlinear partial differential equation model. Hence, various theoretical approaches may be brought to bear on these ODEs.

There are situations [11, 23–25] where this approach is appropriate, particularly where the dynamics of various active or dissipative systems is primarily governed by localized coherent structures such as pulses (solitary waves) and kinks (fronts or shocks). Such coherent structures could also be information carriers, such as in Optics. Since such structures correspond to spatial modulations, they are also often referred to spatially–localized "patterns". The speeds and locations of the coherent structures may vary in a complex manner as they interact, but their spatial coherence is preserved in such situations. It is tempting to apply this approach to any system which admits pulse and/or kink solutions, but caution is necessary. Coherent structures may be transitory when they are unstable to small disturbances in their neighborhood. Also, only some of them may be actually selected, due to such stability considerations.

Another relevant feature of dissipative systems is that they include energy exchange with external sources. Such systems are no longer Hamiltonian, and the solitons in these systems are also qualitatively different from those in Hamiltonian systems. In Hamiltonian systems, soliton solutions appear as a result of balance between diffraction (dispersion) and nonlinearity. Diffraction spreads a beam while nonlinearity will focus it and make it narrower. The balance between the two results in stationary solitary wave solutions, which usually form a one parameter family. In dissipative systems with gain and loss, in order to have stationary solutions, the gain and loss must be also balanced. This additional balance results in solutions which are fixed. Then the shape, amplitude and the width are all completely fixed by the parameters of the dissipative equation. This situation is shown schematically in Fig. 1. However, the solitons, when they exist, can again be considered as "modes" of dissipative systems just as for nondissipative ones.

To briefly recapitulate, the numerical results on dissipative solitons [20, 26] indicate:

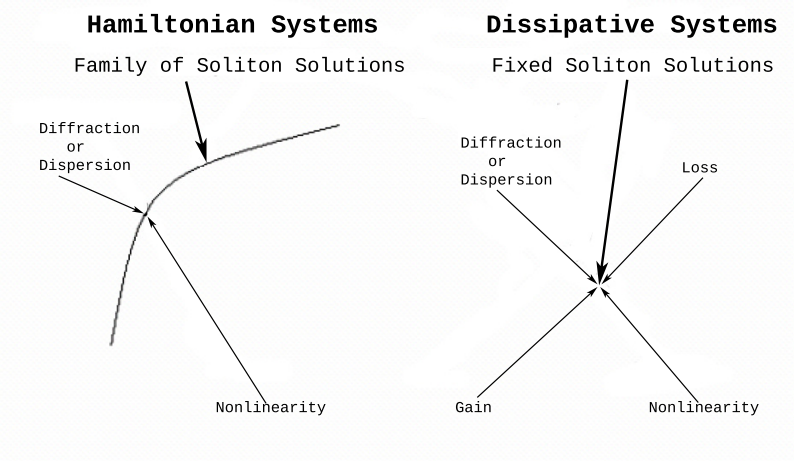

Figure 1: Qualitative difference between the soliton solutions in Hamiltonian and dissipative systems

(a) five new classes of stable amplitude modulated solutions unique to dissipative systems, and
(b) interesting bifurcation sequences of these solutions as parameters are varied.

In addition, a question of great interest [26] is the effect of the system parameters viz. dispersion/nonlinearity/linear and nonlinear gain and loss/spectral filtering on both the structure and the stability of these new classes of dissipative solitons. This last feature was repeatedly mentioned by many speakers in the multi–day session on Dissipative Solitons at the 4^{th} IMACS Conference on Nonlinear Waves held in Athens, Georgia in April 2005.

The above then defines the main themes to be explored in this paper. We focus on the issues of central interest in the area, i.e., the conditions for the occurrence of the five categories of dissipative solitons, as well the dependence of both their shape and their stability on the nonlinearity, dispersion, linear and nonlinear gain, loss and spectral filtering parameters.

In the language of the Los Alamos school, the fully spatiotemporal approach followed here may be said to be the "collective coordinates" formulation. In other words, we consider a pulse or solitary wave at any time as a coherent collective entity (or coordinate). This solitary wave is then temporally modulated. The spatial approach proposed, and explored, in this paper is the variational method. However, the method is very significantly and non–trivially generalized from all earlier applications to deal with our novel classes of dissipative solitary waves. We are very grateful to David Kaup, Jianke Yang and Roberto Camassa for discussions on these formulations.

We would also like to particularly cite David Kaup's recent work, talks and conversations stressing the power, versatility and accuracy of the variational technique in constructing regular and embedded solitons of various complicated $\chi^2 - \chi^3$ systems. These were instrumental in focusing our attention on this method, and attempting to extend its use to new classes of dissipative solitons. Given this setting, in Section §3 we develop and discuss a variational formalism within which to explore the various classes of dissipative solitons. As mentioned, this is significantly generalized over earlier formulations in several crucial ways. Firstly, the starting formulations for the Lagrangian are recent [27] and not well explored.

Also, after extensive discussions with David Kaup, the trial functions have been generalized considerably over conventional ones to keep the shape relatively simple (and the trial function integrable!) while allowing arbitrary temporal variation of the amplitude, width, position, speed and phase of the pulse. In addition, the resulting Euler–Lagrange equations are treated in a completely novel way. Rather than consider on the stable fixed points which correspond to the well–known stationary solitons or plain pulses, we use dynamical systems theory to focus on more complex attractors viz. periodic, quasiperiodic, and chaotic ones. Periodic evolution of the trial function parameters on a stable periodic attractor would yield solitons whose amplitudes are non–stationary or time dependent. In particular, pulsating, snaking (and less easily, creeping) dissipative solitons may be treated using stable periodic attractors of various trial function parameters. Chaotic evolution of the trial function parameters would yield chaotic solitary waves. This approach fails only to address the fifth class of dissipative solitons, viz. exploding or erupting solitons.

The remainder of this paper is organized as follows. In Section §2 we elucidate the new mechanism responsible for the various classes of pulsating solitary wave solutions in dissipative systems, viz. the possibility of Hopf bifurcations. This also explains the absence of pulsating solitary waves in Hamiltonian and integrable systems. Section §3 details the recent variational formulation for dissipative systems, as well as the novel generalized trial functions to be employed in modeling the pulsating solitary waves. Hopf bifurcations in the Euler–Lagrange equations of Section §3 are detailed in Section §4. Periodic evolution of the trial function parameters on stable periodic attractors resulting from supercritical Hopf bifurcations, when substituted back into the trial function, yield pulsating solitary waves. Within this framework, we also comprehensively explore: a. the cascade of period doubling bifurcations observed in the simulations of the CGLE, and b. the effect of the various parameters in the CGLE on the shape (amplitude, width and period) and domain of existence of the pulsating solitary waves. Sections §5 and §6 discuss extensive numerical results for the plain pulsating solitons, and Section §7 summarizes the results and conclusions.

Various other topics concerning solutions of the CGLE have also been considered recently [28–36].

2 Nonexistence of Hopf Bifurcations in Hamiltonian Systems: Connections to Pulsating Solitons

We shall consider the cubic–quintic CGLE in the form [11]

$$\partial_t A = \epsilon A + (b_1 + ic_1)\partial_x^2 A - (b_3 - ic_3)|A|^2 A - (b_5 - ic_5)|A|^4 A \tag{2.1}$$

noting that any three of the coefficients (no two of which are in the same term) may be set to unity by appropriate scalings of time, space and A.

It is widely reported [21, 37] and generally accepted that Hamiltonian systems, as well as integrable systems which are a subclass, do not admit pulsating solitary wave solutions. If excited initially, pulsating solitons in Hamiltonian and integrable systems re–shape themselves and evolve into regular stationary waves. The only exceptions are pulsating structures comprising nonlinear superpositions of stationary solitons in integrable systems [22].

In addition, the regimes of the pulsating solitons in the CGLE are very far from the integrable nonlinear Schrödinger equation limit. This fact, and the great diversity of pulsating solitons in the CGLE, both indicate a new mechanism which is operative in dissipative systems in the creation of these pulsating structures.

The primary point of this paper is that Hopf bifurcations are the new mechanism responsible for the occurrence of these pulsating solitons in dissipative systems, and we shall analyze both plain pulsating solitons and snakes via this mechanism. However, in order to establish that Hopf bifurcations are indeed the operative mechanism creating the various pulsating solitons in dissipative systems, we first proceed to prove their absence in Hamiltonian systems. This will also explain the above–mentioned absence of pulsating solitons in Hamiltonian and integrable systems.

For a Hamiltonian system with Hamiltonian H, the particular evolution equations may be represented in canonical form as [38].

$$\begin{aligned} i\Psi_\zeta &= \frac{\delta H}{\delta \Psi^\star} \\ i\Psi^\star_\zeta &= -\frac{\delta H}{\delta \Psi}. \end{aligned} \tag{2.2}$$

These may be further combined into

$$i\dot{\vec{x}} = L\nabla_{\vec{x}} H(\vec{x}) \tag{2.3}$$

where $\dot{}$ denotes $\delta/\delta\zeta$,

$$\vec{x} = [\Psi, \Psi^\star], \tag{2.4}$$

I is the $n \times n$ unit matrix, and L is the symplectic gradient of $H(\vec{x})$

$$L = \begin{pmatrix} 0 & I \\ -I & 0 \end{pmatrix}. \tag{2.5}$$

Equation (2.3) follows from

$$i \begin{pmatrix} \dot{\Psi} \\ \dot{\Psi}^\star \end{pmatrix} = \begin{pmatrix} 0 & I \\ -I & 0 \end{pmatrix} \begin{pmatrix} \nabla_\Psi H \\ \nabla_{\Psi^\star} H \end{pmatrix}$$

which is identical to (2.2).

The fixed (or equilibrium or critical) points of (2.3) satisfy

$$\nabla_{\vec{x}} H(\vec{x}) = 0, \tag{2.6}$$

or equivalently

$$\frac{\delta H}{\delta \Psi^\star} = 0, \qquad \frac{\delta H}{\delta \Psi} = 0.$$

Using the standard representation

$$H = \frac{1}{2}\langle \Psi_\zeta, \Psi_\zeta \rangle + V(\Psi) \tag{2.7}$$

for the Hamiltonian, this implies

$$\vec{\nabla}_{\Psi} V = 0$$

or

$$\frac{\delta V}{\delta \Psi} = 0. \tag{2.8}$$

At a fixed point $\vec{x}_0 = [\Psi_0, \Psi_0{}^{\star}]$, the Jacobian matrix of (2.3) is

$$J(\vec{x}_0) = L\mathcal{H} \tag{2.9}$$

where

$$\mathcal{H} \equiv \left[\frac{\delta^2 H}{\delta x_i \delta x_j} \right]_{\vec{x}_0} = \begin{pmatrix} \mathcal{V} & 0 \\ 0 & I \end{pmatrix} \tag{2.10}$$

from (2.7). Here

$$\mathcal{V} = \left[\frac{\delta^2 V}{\delta \Psi_i \delta \Psi_j} \right]_{\vec{x}_0} \tag{2.11}$$

Hence, we have

$$J(\vec{x}_0) = \begin{pmatrix} 0 & I \\ -I & 0 \end{pmatrix} \begin{pmatrix} \mathcal{V} & 0 \\ 0 & I \end{pmatrix} = \begin{pmatrix} 0 & I \\ -\mathcal{V} & 0 \end{pmatrix} \tag{2.12}$$

whose eigenvalues λ satisfy the characteristic equation

$$|\mathcal{V} + \lambda^2 I| = 0 \tag{2.13}$$

Since the matrix $\mathcal{V}$ is symmetric, its eigenvalues are real and the solutions λ of (2.13) are thus either real or purely imaginary. Thus, as claimed earlier, Hopf bifurcations cannot occur in Hamiltonian systems. The introduction of dissipation allows the occurrence of Hopf bifurcation and, as we shall model in the remainder of this paper, introduces the various pulsating solitary wave structures which occur in the CGLE.

3 The Generalized Variational Formulation

In this section we develop a general variational formulation to address the pulsating solitons on all parameter ranges. As mentioned earlier, we shall need to generalize previous variational approaches in several crucial ways.

First, the starting formulation of the Lagrangian for dissipative NLPDEs is relatively of recent vintage [27] and neither widely known or widely explored. We are grateful to David Kaup for digging into his encyclopedic body of work and pointing us to this. An alternative, complex formulation of the Lagrangian for dissipative NLPDEs has been recently employed by Skarka [39] to investigate conventional stationary solitons only.

3.1 Formulation

Proceeding as in [27], the Lagrangian for the cubic–quintic CGLE (2.1) may be written as

$$\begin{aligned}\mathcal{L} = r^*\big[\partial_t A - \epsilon A - (b_1 + ic_1)\partial_x^2 A + (b_3 - ic_3)|A|^2 A + (b_5 - ic_5)|A|^4 A\big] \\ + r\big[\partial_t A^* - \epsilon A^* - (b_1 - ic_1)\partial_x^2 A^* + (b_3 + ic_3)|A|^2 A^* + (b_5 + ic_5)|A|^4 A^*\big]\end{aligned} \tag{3.1}$$

Here r is the usual auxiliary equation employed in [27] and it satisfies a perturbative evolution equation dual to the CGLE with all non–Hamiltonian terms reversed in sign.

The second key assumption involves the trial functions $A(t)$ and $r(t)$ which have been generalized considerably over conventional ones to keep the shape relatively simple and the trial functions integrable. To this end, we choose single–humped trial functions of the form:

$$A(x,t) = A_1(t)e^{-\sigma_1(t)^2[x-\phi_1(t)]^2}e^{i\alpha_1(t)} \tag{3.2}$$

$$r(x,t) = e^{-\sigma_2(t)^2[x-\phi_2(t)]^2}e^{i\alpha_2(t)} \tag{3.3}$$

Here, the $A_1(t)$ is the amplitude, the $\sigma_i(t)$'s are the inverse widths, $\phi_i(t)$'s are the positions (with $\phi_i(t)/t$ being phase speeds, $\dot{\phi}_i(t)$ the speed) and $\alpha_i(t)$'s are the phases of the solitons. All are allowed to vary arbitrarily in time. For now, the chirp terms are omitted for simplicity. Substituting (3.2)/(3.3) in (3.1) the effective or averaged Lagrangian is

$$\begin{aligned}L_{EFF} = \int_{-\infty}^{\infty}\mathcal{L}dx = 2\sqrt{\pi}\Bigg\{ - \frac{e^{-\frac{\sigma_1(t)^2\sigma_2(t)^2[\phi_1(t)-\phi_2(t)]^2}{\sigma_1(t)^2+\sigma_2(t)^2}}}{[\sigma_1(t)^2+\sigma_2(t)^2]^{\frac{1}{2}}}\epsilon A_1(t)\cos[\alpha_1(t)-\alpha_2(t)] \\ + \frac{e^{-\frac{3\sigma_1(t)^2\sigma_2(t)^2[\phi_1(t)-\phi_2(t)]^2}{3\sigma_1(t)^2+\sigma_2(t)^2}}}{\Big[3\sigma_1(t)^2+\sigma_2(t)^2\Big]^{\frac{1}{2}}}A_1(t)^3\Big[b_3\cos[\alpha_1(t)-\alpha_2(t)] + c_3\sin[\alpha_1(t)-\alpha_2(t)]\Big] \\ + \frac{e^{-\frac{5\sigma_1(t)^2\sigma_2(t)^2[\phi_1(t)-\phi_2(t)]^2}{5\sigma_1(t)^2+\sigma_2(t)^2}}}{\Big[5\sigma_1(t)^2+\sigma_2(t)^2\Big]^{\frac{1}{2}}}A_1(t)^5\Big[b_5\cos[\alpha_1(t)-\alpha_2(t)] + c_5\sin[\alpha_1(t)-\alpha_2(t)]\Big] \\ + \frac{e^{-\frac{\sigma_1(t)^2\sigma_2(t)^2[\phi_1(t)-\phi_2(t)]^2}{\sigma_1(t)^2+\sigma_2(t)^2}}}{\Big[\sigma_1(t)^2+\sigma_2(t)^2\Big]^{\frac{5}{2}}}\Bigg[\cos[\alpha_1(t)-\alpha_2(t)][\sigma_1(t)^2+\sigma_2(t)^2]^2\dot{A}_1(t) \\ + A_1(t)\Bigg(- 2\sigma_1(t)^2\sigma_2(t)^2\Big[b_1\cos[\alpha_1(t)-\alpha_2(t)] - c_1\sin[\alpha_1(t)-\alpha_2(t)]\Big]\Big[- \sigma_2(t)^2 \\ + \sigma_1(t)^2[-1+2\sigma_2(t)^2[\phi_1(t)-\phi_2(t)]^2]\Big] - \dot{\alpha_1}(t)\sin[\alpha_1(t)-\alpha_2(t)][\sigma_1(t)^2+\sigma_2(t)^2]^2 \\ - \sigma_1(t)\dot{\sigma_1}(t)\cos[\alpha_1(t)-\alpha_2(t)]\Big[\sigma_1(t)^2+\sigma_2(t)^2+2\sigma_2(t)^4[\phi_1(t)-\phi_2(t)]^2\Big] \\ - 2\dot{\phi_1}(t)\sigma_1(t)^2\sigma_2(t)^2[\phi_1(t)-\phi_2(t)][\sigma_1(t)^2+\sigma_2(t)^2]\cos[\alpha_1(t)-\alpha_2(t)]\Bigg)\Bigg]\Bigg\}\end{aligned} \tag{3.4}$$

Since (3.4) reveals that only the relative phase $\alpha(t) = \alpha_1(t) - \alpha_2(t)$ of $A(x,t)$ and $r(x,t)$

is relevant, we henceforth take

$$\begin{aligned}\alpha_1(t) &= \alpha(t)\\ \alpha_2(t) &= 0\end{aligned} \tag{3.5}$$

with no loss of generality.

Also, for algebraic tractability, we have found it necessary to assume

$$\sigma_2(t) = m\sigma_1(t) \equiv m\sigma(t). \tag{3.6}$$

While this ties the widths of the $A(x,t)$ and $r(x,t)$ fields together, the loss of generality is acceptable since the field $r(x,t)$ has no real physical significance.

For reasons of algebraic simplicity, we may also scale the positions according to:

$$\begin{aligned}\phi_1(t) &= \phi(t)\\ \phi_2(t) &= 0,\end{aligned} \tag{3.7}$$

although this assumption may easily be relaxed. In fact, we may expect that it may be necessary to relax (3.7) for certain classes of dissipative solitons.

Finally, for real solutions (note that the numerical results in [20, 26] pertain to $|A(x,t)|$), we may make the additional assumption

$$\alpha(t) = 0 \tag{3.8}$$

when desired, although this too may be easily relaxed.

Hence, using all assumptions, (i.e. (3.5)–(3.7) in (3.4)), the effective Lagrangian (3.4) may be written in a simpler but still general form

$$\begin{aligned}L_{EFF} \;=\; 2\sqrt{\pi}\Bigg\{ \frac{A_1(t)}{\sigma(t)}\Bigg[&-\frac{e^{-\frac{m^2\sigma(t)^2\phi(t)^2}{1+m^2}}}{[1+m^2]^{\frac{1}{2}}}\epsilon\cos\alpha(t)\\ &+\frac{e^{-\frac{3m^2\sigma(t)^2\phi(t)^2}{3+m^2}}}{[3+m^2]^{\frac{1}{2}}}A_1(t)^2\Big[b_3\cos\alpha(t)+c_3\sin\alpha(t)\Big]\\ &+\frac{e^{-\frac{5m^2\sigma(t)^2\phi(t)^2}{5+m^2}}}{[5+m^2]^{\frac{1}{2}}}A_1(t)^4\Big[b_5\cos\alpha(t)+c_5\sin\alpha(t)\Big]\Bigg]\\ &+\frac{e^{-\frac{m^2\sigma(t)^2\phi(t)^2}{1+m^2}}}{[1+m^2]^{\frac{5}{2}}\sigma(t)^2}\Bigg[(1+m^2)^2\cos\alpha(t)\sigma(t)\dot{A}_1(t)\\ &-A_1(t)\Bigg(4m^4\sigma(t)^5\phi(t)^2\Big[b_1\cos\alpha(t)-c_1\sin\alpha(t)\Big]\\ &+(1+m^2)^2\sigma(t)\dot{\alpha}(t)\sin\alpha(t)+(1+m^2)\dot{\sigma}(t)\cos\alpha(t)\\ &-2m^2(1+m^2)\sigma(t)^3\Big[b_1\cos\alpha(t)-c_1\sin\alpha(t)\Big]\\ &+2m^4\dot{\sigma}(t)\sigma(t)^2\phi(t)^2+\dot{\phi}(t)\phi(t)\cos\alpha(t)\Bigg)\Bigg]\Bigg\}\end{aligned} \tag{3.9}$$

4 Framework for Investigation of Euler–Lagrange Equations for Pulsating Solitons

4.1 Variational Equations

For plain pulsating solitons, the speed is always zero [20, 26] and we take

$$\phi_1(t) = \phi_2(t) = 0. \tag{4.1}$$

However, we need not, in general invoke (3.8), since the solution of (2.1) must be complex. Therefore, the trial functions (3.2) and (3.3) become

$$A(x,t) = A_1(t)e^{-\sigma(t)^2x^2}e^{i\alpha(t)} \tag{4.2}$$

$$r(x,t) = e^{-\sigma(t)^2} \tag{4.3}$$

Substituting the last two equations into (3.9), and by choosing $m = 1$, the simplified effective Lagrangian becomes

$$\begin{aligned} L_{EFF} \;=\; & \frac{\sqrt{\pi}}{6\sigma(t)^2}\Bigg[6A_1(t)^3\sigma(t)\big(b_3\cos\alpha(t) + c_3\sin\alpha(t)\big) \\ & +\sqrt{2}\Bigg(2\sqrt{3}A_1(t)^5\sigma(t)\big(b_5\cos\alpha(t) + c_5\sin\alpha(t)\big) \\ & +6\dot{A}_1(t)\sigma(t)\cos\alpha(t) - 6A_1(t)\sigma(t)\sin\alpha(t)\big(c_1\sigma(t)^2 + \dot{\alpha}(t)\big) \\ & -3A_1(t)\cos\alpha(t)\big(\dot{\sigma}(t) + 2\epsilon\sigma(t) - 2b_1\sigma(t)^3\big)\Bigg)\Bigg] \end{aligned} \tag{4.4}$$

We are left with three parameters $A_1(t)$, $\sigma(t)$ and $\alpha(t)$ in L_{EFF}. Varying these parameters (3.4), we obtain

$$\frac{\partial L_{EFF}}{\partial \star\,(t)} - \frac{\mathrm{d}}{\mathrm{dt}}\Big(\frac{\partial L_{EFF}}{\partial \dot{\star}(t)}\Big) = 0,$$

where $\star$ refers to A_1, σ, or α. Solving for $\dot{\star}(t)$ as a system of three equations,

$$\begin{aligned} \dot{A}_1(t) &= f_1[A_1(t), \sigma(t), \alpha(t)] \\ \dot{\sigma}(t) &= f_2[A_1(t), \sigma(t), \alpha(t)] \\ \dot{\alpha}(t) &= f_3[A_1(t), \sigma(t), \alpha(t)], \end{aligned} \tag{4.5}$$

where the f_i are complicated nonlinear functions of the arguments.

4.2 Hopf Bifurcations

The general strategy for investigating pulsating solitons and their bifurcations within the variational framework is as follows. The Euler–Lagrange equations (4.5) are treated in a completely novel way. Rather than consider the stable fixed points which correspond to the

well–known stationary solitons or plain pulses, we use Hopf bifurcation theory to focus on periodic attractors. Periodic evolution of the trial function parameters on stable periodic attractors yield the pulsating soliton whose amplitude is non–stationary or time dependent.

We derive the conditions for the temporal Hopf bifurcations of the fixed points. The conditions for supercritical temporal Hopf bifurcations, leading to stable periodic orbits of $A_1(t)$, $\sigma(t)$, and $\alpha(t)$ may be evaluated using the method of Multiple Scales. These are the conditions or parameter regimes where exhibit stable periodic oscillations, and hence stable pulsating solitons will exist within our variational formulation. Note that, as is easy to verify numerically, periodic oscillations of $A_1(t)$, $\sigma(t)$, and $\alpha(t)$, correspond to a spatiotemporal pulsating soliton structure of the $|A(x,t)|$ given by (3.2).

The fixed points of (4.5) are given by a complicated system of transcendental equations. These are solved numerically to obtain results for each particular case.

For a typical fixed point, the characteristic polynomial of the Jacobian matrix of a fixed point of (4.5) may be expressed as

$$\lambda^3 + \delta_1\lambda^2 + \delta_2\lambda + \delta_3 = 0 \tag{4.6}$$

where δ_i with $i = 1...3$ depend on the system parameters and the fixed points. Since these are extremely involved, we omit the actual expressions, and evaluate them numerically where needed.

To be a stable fixed point within the linearized analysis, all the eigenvalues must have negative real parts. Using the Routh–Hurwitz criterion, the necessary and sufficient conditions for (4.6) to have $Re(\lambda_{1,2,3}) < 0$ are:

$$\delta_1 > 0, \quad \delta_3 > 0, \quad \delta_1\delta_2 - \delta_3 > 0. \tag{4.7}$$

On the contrary, one may have the onset of instability of the plane wave solution occurring in one of two ways. In the first, one root of (4.5) (or one eigenvalue of the Jacobian) becomes non–hyperbolic by going through zero for

$$\delta_3 = 0. \tag{4.8}$$

Equation (4.8) is thus the condition for the onset of "static" instability of the plane wave. Whether this bifurcation is a pitchfork or transcritical one, and its subcritical or supercritical nature, may be readily determined by deriving an appropriate canonical system in the vicinity of (4.8) using any of a variety of normal form or perturbation methods.

One may also have the onset of dynamic instability ("flutter" in the language of Applied Mechanics) when a pair of eigenvalues of the Jacobian become purely imaginary. The consequent Hopf bifurcation at

$$\delta_1\delta_2 - \delta_3 = 0 \tag{4.9}$$

leads to the onset of periodic solutions of (4.5) (dynamic instability or "flutter").

4.3 Effects of system parameters on shape of the Pulsating Soliton

Also, within the regimes of stable periodic solutions, we comprehensively investigate:

a. the effects of the nonlinearity/dispersion/linear and nonlinear gain/loss spectral filtering on the shape and structure of the pulsating solitons given by (3.2), and

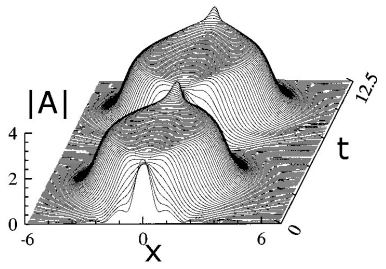

Figure 2: Plain pulsating soliton that shows period doubling, $b_3 = -0.785$

b. the period doubling sequences of the pulsating solitons given by (3.2) as the above system parameters are varied.

To study the effects of system parameters on the shape and the stability of the Pulsating Soliton, we integrate (4.2)–(4.3) numerically in Mathematica for different sets of the various system parameters within the regime of stable periodic solutions. The resulting periodic time series for $A_1(t)$, $\sigma(t)$ and $\alpha(t)$ and are then simply inserted in (3.2) whose spatiotemporal structure ($|A(x,t)|$ versus x and t) may be plotted. As the various system parameters within the stable regime are varied, the effects of the pulsating soliton amplitude, width, and phase will be studied.

4.4 Investigation of period doubling

Pulsating solitons can exhibit more complicated behaviors as one of the parameters changes. Simple pulsations can be transformed by period doubling and period quadrupling as the parameter changes further. This phenomena occurs due to the bifurcations at certain boundaries in the parameter space.

To study the period doubling bifurcation sequences of the pulsating solitons, we will use the standard numerical diagnostics [40]. In other words, a stable pulsating soliton will be constructed as above for a set of parameters in the stable regime. One parameter (the "distinguished bifurcation parameter") will then be varied and the effect on the periodic orbits for $A_1(t)$, $\sigma(t)$ and $\alpha(t)$ will be studied. If these period double (or subharmonics appear in the power spectral density [40]), note that this would result in an approximate temporal period doubling of $|A(t)|$ given by (3.2). This is precisely what is observed in the numerical simulations of Akhmediev et al [20], as we can see in Figures 2 and 3. In his simulations, as b_3 is varied the plane pulsating soliton experienced almost period doubling. Further varying of b_3 produced almost period quadrupling.

In the next Section we shall implement the above procedure and also will make detailed comparisons between our work that of Akhmediev et al [20, 26].

5 Results for the General Plane Pulsating Soliton

An example of a plain pulsating soliton, obtained by us via independent simulations on (2.1), is shown in Figure 4 using the trial functions (4.2) and (4.3). It has a different shape at each time t, since it evolves, but it recovers its exact initial shape after a period.

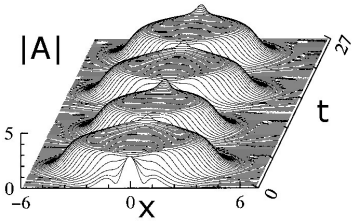

Figure 3: Plain pulsating soliton that shows period quadrupling, $b_3 = -0.793$

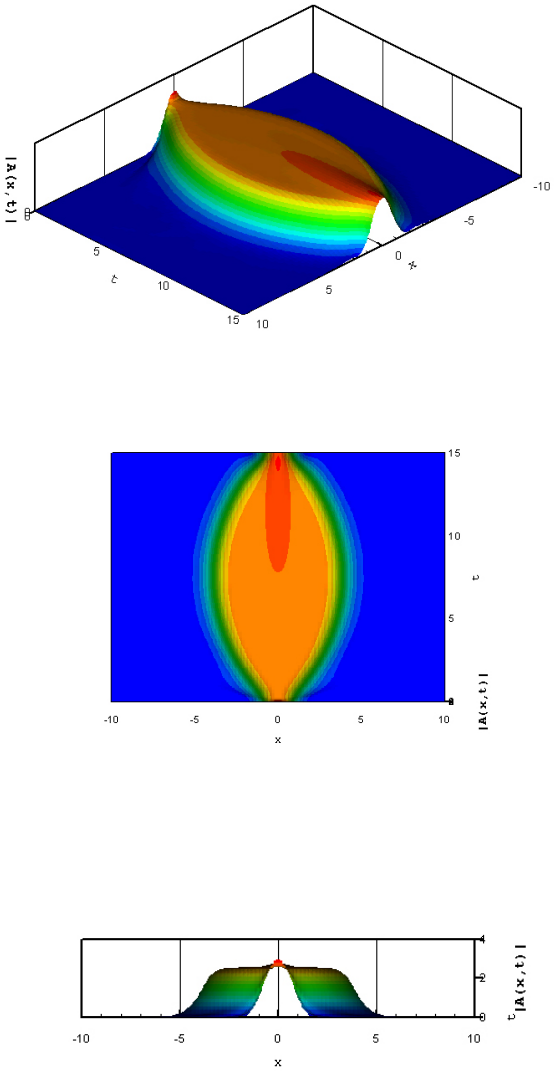

Figure 4: Plain pulsating soliton for $b_3 = -0.66$ and $\epsilon = -0.1$

To derive the conditions for occurrence of stable periodic orbits of $A_1(t)$, $\sigma(t)$, and $\alpha(t)$, we proceed as follows.

First, we fix a set of system parameters $b_1 = 0.08$, $b_5 = 0.1$, $c_1 = 0.5$, $c_3 = 1$, $c_5 = -0.1$. Then, we solve numerically the system of transcendental equations (4.5), which are the equations of the fixed points. By the Ruth–Hurwitz conditions, the Hopf curve is defined as $\delta_1\delta_2 - \delta_3 = 0$. This condition, along with the equations of the fixed points leads to onset of periodic solutions of (4.5) as we will see next.

On the Hopf bifurcation curve we obtain that $b_3 = -0.216825$, and $\epsilon = -0.345481$, while the fixed points are $A_1(0) = 0.954712$, $\sigma(0) = 0.917093$, and $\alpha(0) = -0.181274$. Using these values of b_3 and ϵ , we integrate numerically the systems of 3 ODEs (4.5), using as initial conditions the three values of the fixed points. Hopf bifurcations occur in this system leading to periodic orbits.

Next, we may plot the time series of the periodic orbit for the amplitude $A_1(t)$, and, as expected, we noticed that the amplitude was very small, since it is proportional to the square root of the distance from the Hopf curve.

To construct pulsating solitons with amplitudes large enough, we had to move away from the Hopf curve, as much as possible, but at the same time to be sure not to be outside of the parameters ranges for the existence of the pulsating soliton. That could be achieved by varying one or more of the system parameters. First, we varied ϵ slowly away from the Hopf curve. Repeating the above procedure to construct a plane pulsating soliton, we noticed that the pulsating soliton still had very small amplitudes $A_1(t)$, of magnitude only of 10^{-4}. Therefore, we decided to vary another parameter, b_3, which stands for the cubic gain when negative. We found that the domain of existence for the pulsating soliton as a function of b_3 was $[-0.2531943, -0.1424]$, passing through the Hopf curve value of $b_3 = -0.216825$. Within this range, we varied b_3, and studied the effects on the shape and the stability, as well as the various bifurcations that lead potentially to period doubling and quadrupling. For the largest value of b_3, i.e. $b_3 = -0.1424$, we numerically integrate in Mathematica the three differential equations (4.5), and we plot the periodic orbit, which is shown in Figure 5.

The resulting periodic time series for $A_1(t)$, $\sigma(t)$, and $\alpha(t)$ from Figure 6 are then simply inserted in (4.2) whose spatiotemporal structure ($|A(x,t)|$ or phase $A(x,t)$ versus x and t) is plotted in Figure 7. As the various system parameters c_1, c_3, c_5, b_1, b_5 within the stable regime are varied, the effects of the pulsating soliton amplitude, width, position, phase speed (and, less importantly, phase) may also be studied, and this is discussed subsequently.

Repeating the above, we also show the orbit and the plane pulsating soliton for the smallest value of $b_3 = -0.2531943$ in Figures 8 and 9.

Next, we consider the detailed effects of varying the parameter b_3. For the chosen values of the system parameters of $b_1 = 0.08$, $b_5 = 0.1$, $c_1 = 0.5$, $c_3 = 1$, $c_5 = -0.1$, and $\epsilon = -0.345481$, with the fixed points $A_1(0) = 0.954712$, $\sigma(0) = 0.917093$, and $\alpha(0) = -0.181274$, from (4.5) and (4.9), the Hopf bifurcation occurs at

$$b_{3Hopf} = -0.216825 \tag{5.1}$$

First, let us consider values of b_3 greater that b_{3Hopf}. There is a stable and robust periodic orbit to this side which becomes larger and deforms as b_3 is increased up to -0.1424. A representative periodic orbit is in Figure 5.

Next, moving to values smaller than b_{3Hopf}, we see a clean, periodic orbit which slowly

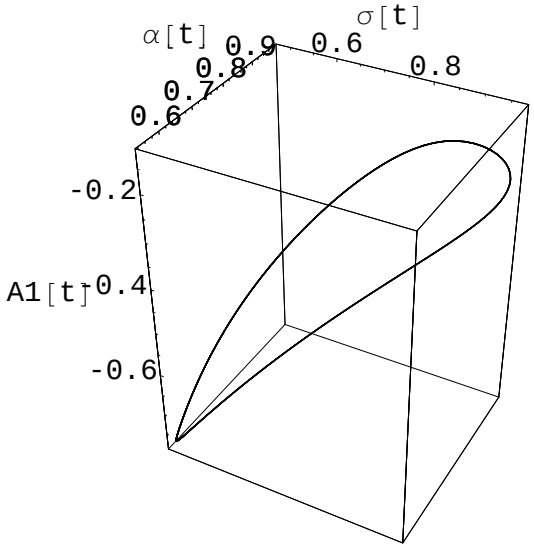

Figure 5: The periodic orbit for $b_3 = -0.1424$

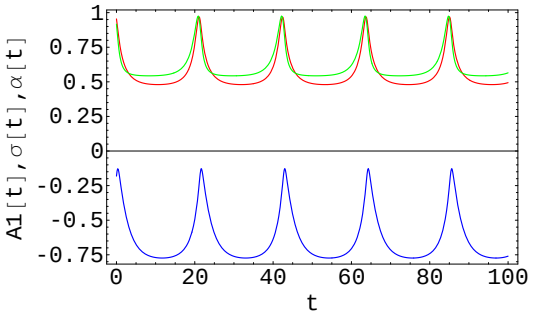

Figure 6: Periodic time series for $b_3 = -0.1424$

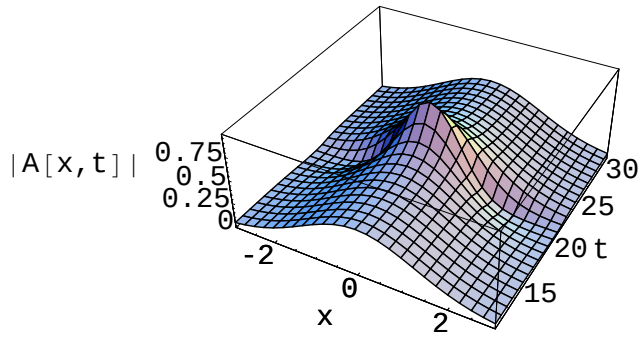

Figure 7: Plane pulsating soliton for $b_3 = -0.1424$

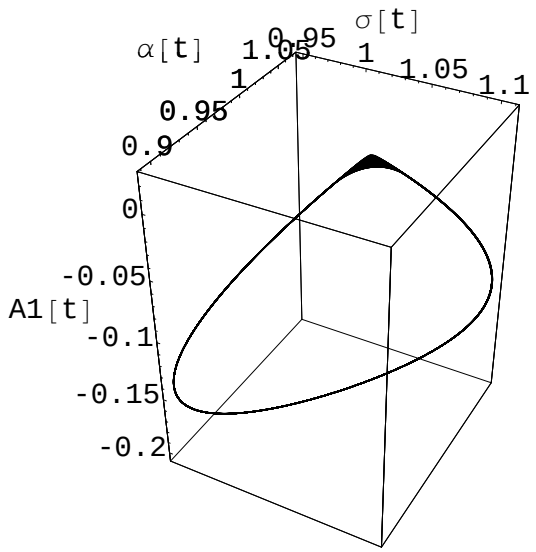

Figure 8: The periodic orbit for $b_3 = -0.2531943$

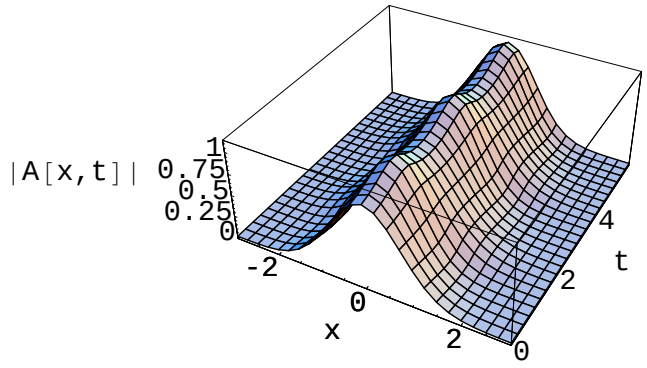

Figure 9: Plane pulsating soliton for $b_3 = -0.2531943$

grows in size as b_3 is made more negative. The periodic orbit, time series, and solitary waves are qualitatively similar to those for $b_3 > b_{3Hopf}$.

However, more interesting dynamics is seen as b_3 is decreased further. The periodic orbit goes unstable via a very rapid, complete cascade of period–doubling bifurcations between $b_3 = -0.25$, and $b_3 = -0.2516$. In Figure 10 we show the period doubled orbit for $b_3 = -0.2516$. The orbit at $b_3 = -0.2531943$ after many more period doublings is shown in Figure 8. The corresponding solitary wave solution is shown in Figure 9. Notice that this feature agrees with the sequence of period doublings for pulsating solitons seen by Akhmediev et al [20]. Note also that one may track the complete cascade of period doublings using software such AUTO or DERPER, or using the schemes of Holodniok and Kubicek [41].

Next, we shall consider the effect of all the various parameters in the CGLE (2.1) on the shape (amplitude, width, period) and stability of the pulsating solitary wave. This is a key feature of interest that was repeatedly mentioned by many speakers in the multi–day session on Dissipative Solitons at the 4$^{\text{th}}$ IMACS Conference on Nonlinear Waves held in Athens, Georgia in April 2005, as there are no existing theoretical guidelines or predictions about this at all.

In considering the parameter effects on the solitary wave shape and period, note that the wave is a spatially coherent structure (or a "collective coordinate" given by the trial function) whose parameters oscillate in time. Hence, the temporal period of the pulsating soliton is the same as the period T of the oscillations of $A_1(t)$, $\sigma(t)$, and $\alpha(t)$ on their limit cycle. As for the peak amplitude and peak width of the pulsating wave, these are determined by the peak amplitude A_{1p} of $A_1(t)$, and the reciprocal of the peak amplitude σ_p of $\sigma(t)$ respectively, i.e. at any time t when the amplitude is maximum, the width will be minimum, and vice versa.

Keeping the above in mind, we vary the parameters of the CGLE in turn and we observe the resulting effects on A_{1p} (the peak amplitude), σ_p (the inverse width), and T (the temporal period) of the pulsating soliton:

a. For increased b_1, the values of A_{1p}, σ_p, and T all increase.

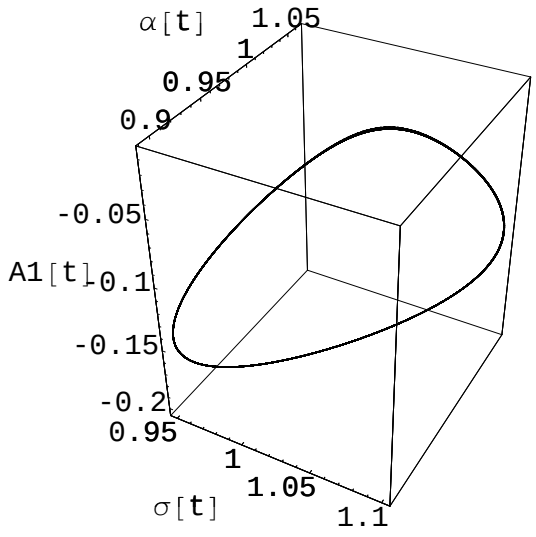

Figure 10: The periodic orbit for $b_3 = -0.2516$

b. Increasing b_5 augments all of A_{1p}, σ_p, and T.

c. Raising c_1 increases A_{1p}, σ_p, and T.

d. Incrementing c_3 decreases all of A_{1p}, σ_p, and T.

e. Augmenting c_5 causes a decrease in A_{1p}, σ_p, and T.

f. Raising ϵ causes A_{1p}, σ_p, and T to fall.

The above constitute our detailed predictions of the various parameters in the CGLE on the amplitude, inverse width, and temporal width of the pulsating solitons. We have verified that each set of predictions a.–f. above agree when the corresponding parameter is varied in the solitary wave simulation for the full PDE shown in Figure 4. Note also that $A_1(t)$ and $\sigma(t)$ are always in phase, so that A_{1p} and σ_p occur simultaneously. Thus, the pulsating solitons are tallest where they have least width. This is completely consistent with our simulation in Figure 4, as well as those in [20, 21].

Finally, in the next section, we briefly discuss a simpler alternative trial function ansatz.

6 Real Pulsating Solitons

For plain pulsating solutions, the speed is always zero [20, 26]. In attempting to find the simplest trail function ansatz we also invoke (3.8), since we want a real pulsating soliton. Therefore, the trial functions (3.2) and (3.3) become

$$A(x,t) = A_1(t)e^{-\sigma(t)^2 x^2} \tag{6.1}$$

$$r(x,t) = e^{-\sigma(t)^2} \tag{6.2}$$

Substituting the last two equations into (3.9), and by choosing $m = 1$, the simplified effective Lagrangian becomes

$$\begin{aligned} L_{EFF} &= \frac{\sqrt{\pi}}{6\sigma(t)^2}\Bigg(6A_1(t)^3\sigma(t)b_3 + \sqrt{2}\Bigg(2\sqrt{3}A_1(t)^5\sigma(t)b_5 \\ &\quad +6\dot{A}_1(t)\sigma(t) - 3A_1(t)\big(\dot{\sigma}(t) + 2\epsilon\sigma(t) - 2b_1\sigma(t)^3\big)\Bigg)\Bigg) \end{aligned} \tag{6.3}$$

The Euler–Lagrange equations obtained by varying $A_1(t)$, and $\sigma(t)$ parameters are

$$\begin{aligned} &\frac{\partial L_{EFF}}{\partial \sigma(t)} - \frac{\mathrm{d}}{\mathrm{dt}}\Big(\frac{\partial L_{EFF}}{\partial \dot{\sigma}(t)}\Big) = \\ &= -\frac{\sqrt{\pi}}{6\sigma^2(t)}\big[2A_1(t)^3\big(\sqrt{6}b_5A_1(t)^2 + 3b_3\big) \\ &- 6\sqrt{2}A_1(t)\big(\epsilon + b_1\sigma(t)^2\big) + 3\sqrt{2}\dot{A}_1(t)\big] = 0 \end{aligned} \tag{6.4}$$

$$\begin{aligned} &\frac{\partial L_{EFF}}{\partial A_1(t)} - \frac{\mathrm{d}}{\mathrm{dt}}\Big(\frac{\partial L_{EFF}}{\partial \dot{A}_1(t)}\Big) = \\ &= \frac{\sqrt{\pi}}{6\sigma^2(t)}\big[2A_1(t)^2\sigma(t)\big(5\sqrt{6}b_5A_1(t)^2 + 9b_3\big) \\ &- 6\sqrt{2}\sigma(t)\big(\epsilon - b_1\sigma(t)^2\big) + 3\sqrt{2}\dot{\sigma}(t)\big] = 0 \end{aligned} \tag{6.5}$$

Solving the above equations for $\dot{A}_1(t)$, and $\dot{\sigma}(t)$, we obtain

$$\begin{aligned} \dot{A}_1(t) &= -\frac{1}{3}A_1(t)\Big(-6\epsilon + 3\sqrt{2}b_3A_1(t)^2 + 2\sqrt{3}b_5A_1(t)^4 - 6b_1\sigma(t)^2\Big) \\ \dot{\sigma}(t) &= -\frac{1}{3}\sigma(t)\Big(-6\epsilon + 9\sqrt{2}b_3A_1(t)^2 + 10\sqrt{3}b_5A_1(t)^4 + 6b_1\sigma(t)^2\Big) \end{aligned} \tag{6.6}$$

Considering a typical fixed point, the characteristic polynomial of the Jacobian matrix of a fixed point (6.6) may be expressed as

$$\lambda^2 + \delta_1\lambda + \delta_2 = 0 \tag{6.7}$$

where

$$\delta_1 = -4\epsilon + 6\sqrt{2}b_3A_1(t)^2 + \frac{20}{\sqrt{3}}b_5A_1(t)^4 + 4b_1\sigma(t)^2 \tag{6.8}$$

$$\begin{aligned} \delta_2 &= 4\epsilon^2 - 12\sqrt{2}b_3\epsilon A_1(t)^2 + 18b_3^2A_1(t)^4 - \frac{40}{\sqrt{3}}\epsilon A_1(t)^4 + 20\sqrt{6}b_3b_5A_1(t)^6 + \frac{100}{3}b_5^2A_1(t)^8 \\ &\quad -8b_1\epsilon\sigma(t)^2 + 36\sqrt{2}b_1b_3A_1(t)^2\sigma(t)^2 + \frac{200}{\sqrt{3}}b_1b_5A_1(t)^4\sigma(t)^2 - 12b_1^2\sigma(t)^4 \end{aligned} \tag{6.9}$$

From the Routh–Hurwitz conditions, the requirement to have Hopf bifurcation is to have $\delta_1 = 0$ and $\delta_2 > 0$. However, we will show that the real plane pulsating soliton cannot undergo Hopf bifurcation.

At a fixed point of (6.6), we have

$$\begin{aligned} \epsilon &= \sqrt{2}b_3 A_1(t)^2 + \sqrt{3}b_5 A_1(t)^4 \\ \sigma(t)^2 &= -\frac{1}{6b_1}\Big(3\sqrt{2}b_3 A_1(t)^2 + 4\sqrt{3}b_5 A_1(t)^4\Big), \end{aligned} \tag{6.10}$$

and substituting the above into (6.8),(6.9), we obtain

$$\begin{aligned} \delta_1 &= 0 \\ \delta_2 &= -\frac{32}{3}A_1(t)^4\Big(3b_3^2 + 4\sqrt{6}b_3 b_5 A_1(t)^2 + 12b_5^2 A_1(t)^4\Big). \end{aligned} \tag{6.11}$$

Now, it is obvious to see that $\delta_2 \leq 0$ since $3b_3^2 + 4\sqrt{6}b_3 b_5 A_1(t)^2 + 12b_5^2 A_1(t)^4 > 0$ for all $A_1(t)$, because its discriminant $\triangle = -48b_3^2 b_5^2 < 0$. Hence Hopf bifurcation does not occur, probably because the real solution (6.1) is too rudimentary and, in particular, because it represents a real solution.

7 Conclusions and Discussions

In conclusion, we have developed a comprehensive theoretical framework for analyzing the full spatiotemporal structure of pulsating solitary waves in the complex, cubic–quintic Ginzburg–Landau equation. This includes elucidating the mechanism operative in creating these new classes of solitons in dissipative systems, as well as their absence in Hamiltonian and integrable systems where only stationary solitons are observed to occur.

The specific theoretical modeling includes the use of a recent variational formulation and significantly generalized trial function for the solitary waves solutions. In addition, the resulting Euler–Lagrange equations are treated in an entirely different way by looking at their stable periodic solutions (or limit cycles) resulting from supercritical Hopf bifurcations. Oscillations of their trial function parameters on these limit cycles provide the pulsations of the amplitude, width, and phase of the solitons. The model also allows for detailed predictions regarding the other issue of central interest for the pulsating solitons, viz. the effect of each of the system parameters on the amplitude, width, period, and stability of the solitary waves.

Also, given the generality of the theoretical framework developed in this paper, it provides a platform for the detailed modeling of the snake and chaotic solitary waves as well. These are the focus of current work in this area.

Acknowledgment

We would like to acknowledge extremely insightful comments by David Kaup on the variational formulation, as well as on soliton perturbation theory. Helpful inputs were also provided by Jianke Yang (Vermont) and Roberto Camassa (Chapel Hill).

References

[1] R.K. Dodd, J.C. Eilbeck, J.D. Gibbon, and H.C. Morris, *Solitons and Nonlinear Wave Equations*, Academic, London, 1982.

[2] P.G. Drazin and W.H. Reid, *Hydrodynamic Stability*, Cambridge U. Press, Cambridge, 1981.

[3] I.S. Aranson and L.Kramer, *The World of the Complex Ginzburg–Landau Equation*, Rev. Mod. Phys. **74** (2002), 99.

[4] C.Bowman and A.C. Newell, *Natural Patterns and Wavelets*, Rev. Mod. Phys. **70** (1998), 289.

[5] L. Brusch, A. Torcini, and M. Bär, *Nonlinear analysis of the Eckhaus Instability: Modulated amplitude waves and phase chaos*, Phys.D **160** (2001), 127.

[6] L. Brusch, A. Torcini, M. van Hecke, M. G. Zimmermann, and M. Bär, *Modulated amplitude waves and defect formation in the one–dimensional complex Ginzburg–Landau equation*, Phys D. **160** (2001), 127.

[7] L.R. Keefe, *Dynamics of perturbed wavetrain solutions to the Ginzburg–Landau equation*, Stud. Appl. Math. **73** (1985), 91.

[8] M.J. Landman, *Solutions of the GL equation of interest in shear flow*, Stud. Appl. Math. **76** (1987), 187.

[9] P.K. Newton and L. Sirovich, *Instabilities of the Ginzburg–Landau equation: Periodic solutions*, Quart. Appl. Math. **XLIV** (1984), 49.

[10] ———, *Instabilities of the Ginzburg–Landau equation Pt.II: Secondary bifurcations*, Quart. Appl. Math. **XLIV** (1986), 367.

[11] W. van Saarloos and P. C. Hohenberg, *Fronts, pulses, sources and sinks in generalized complex Ginzburg–Landau equation*, Phys.D **56** (1992), 303.

[12] M. van Hecke, C. Storm, and W. van Saarloos, *Sources, sinks and wavenumber selection in coupled CGL equations*, Phys.D **134** (1999), 1.

[13] R. Alvarez, M. van Hecke, and W. van Saarloos, *Sources and sinks separating domains of left– and right–traveling waves: Experiment versus amplitude equations*, Phys.Rev.E **56** (1997), R1306.

[14] P. Holmes, *Spatial structure of time periodic solutions of the GL equation*, Phys.D **23** (1986), 84.

[15] A. Doelman, *Traveling waves in the complex GL equation*, J. Nonlin. Sci **3** (1993), 225.

[16] ———, *Periodic and quasiperiodic solutions of degenerate modulation equations*, Phys.D **53** (1991), 249.

[17] J. Duan and P. Holmes, *Fronts, domain walls and pulses in a generalized GL equation*, Proc. Edin. Math. Soc. **38** (1995), 77.

[18] A. Doelman, *Slow time–periodic solutions of the GL equation*, Phys.D **40** (1989), 156.

[19] J. M. Soto-Crespo, N. Akhmediev, and G. Town, *Interrelation between various branches of stable solitons in dissipative systems*, Optics Comm. **199** (2001), 283.

[20] N. Akhmediev, J. Soto-Crespo, and G. Town, *Pulsating solitons, chaotic solitons, period doubling, and pulse coexistence in mode–locked laser: CGLE approach*, Phys. Rev.E **63** (2001), 56602.

[21] D. Artigas, L. Torner, and N. Akhmediev, *Robust heteroclinic cycles in the one-dimension CGLE*, Opt. Comm. **143** (1997), 322.

[22] J. Satsuma and N. Yajima, *Initial–value problems of one–dimensional self–modulation of nonlinear–waves in dispersive media*, Progr. Theoret. Phys. Suppl. **55** (1974), 284.

[23] P. G. Drazin and R. S. Johnson, *Solitons: an Introduction*, Cambridge U. Press, Cambridge, 1989.

[24] J. D. Murray, *Mathematical Biology*, Springer–Verlag, Berlin, 1989.

[25] N.J. Balmforth, *Solitary waves and homoclinic orbits*, Ann. Rev. Fluid Mechanics **27** (1995), 335.

[26] N. Akhmediev, *Pulsating solitons in dissipative systems*, 2005. 4$^{\text{th}}$ IMACS Conf. on Nonlinear Waves, Athens, Georgia, April 2005.

[27] D.J. Kaup and B.A. Malomed, *The variational principle for nonlinear waves in dissipative systems*, Physica D **87** (1995), 155.

[28] Jin-Liang Zhang, Ming-Liang Wang, and Ke-Quan Gao, *Exact solutions of generalized Zakharov and Ginzburg–Landau equations*, Chaos Solitons Fractals **32** (2007), 1877.

[29] Man Feng Hu and Zhen Yuan Xu, *Spatiotemporal chaotic synchronization for modes coupled two Ginzburg–Landau equations*, Appl. Math. Mech. (English Ed.) **27** (2006), 1149.

[30] B. Marts, A. Hagberg, E. Meron, and A.L. Lin, *Resonant and nonresonant patterns in forced oscillators*, Chaos Solitons Fractals **16** (2006), 037113.

[31] M. Fabrizio, *Ginzburg–Landau equations and first and second order phase transitions*, Internat. J. Engrg. Sci. **44** (2006), 529.

[32] A. Mohamadou, F. Ndzana, and T. F. Cofané, *Pulse solutions of the modified cubic complex Ginzburg–Landau equation*, Phys. Scr. **73** (2006), 596.

[33] Vasily E. Tarasov, *Psi-series solutions of fractional Ginzburg–Landau equation*, J. Phys. A **39** (2006), 8395.

[34] Sergey Yu Vernov, *Painlevé analysis and exact solutions of nonintegrable systems*, Softex, Sofia, 2006.

[35] S. C. Mancas and S. R. Choudhury, *Traveling wavetrains in the complex cubic–quintic Ginzburg–Landau equation*, Chaos Solitons Fractals **28** (2006), 834.

[36] ———, *Bifurcations and competing coherent structures in the cubic–quintic Ginzburg–Landau equation. I. Plane wave (CW) solutions*, Chaos Solitons Fractals **27** (2006), 1256.

[37] N. Akhmediev and A. Ankiewicz, *Dissipative Solitons in the CGLE and Swift–Hohenberg Equations*, Dissipative Solitons, Springer, Berlin, 2005.

[38] L. D. Fadeev and L. A. Takhtajan, *Hamiltonian Methods in the Theory of Solitons*, Springer, Berlin, 1986.

[39] V. Skarka and N. Aleksic, *Generation and dynamics of dissipative spatial solitons*, 2005. 4$^{\text{th}}$ IMACS Conf. on Nonlinear Waves, Athens, Georgia, April 2005.

[40] A. H. Nayfeh and B. Balachandran, *Applied Nonlinear Dynamics*, John Wiley, 1995.

[41] M. Holodniok and M. Kubicek, *Computation of period doubling points in ODEs*, Institut für Mathematik Report TUM-8406, Technic Univ. of München, Germany, 1984.